

Refereed Proceedings

The 13th International Conference on

Fluidization - New Paradigm in Fluidization

Engineering

Engineering Conferences International

Year 2010

UNDERSTANDING CAPTURE
EFFICIENCY IN FLUIDIZED BEDS

K Seng Lim*

Trevor D. Hadley†

Jonian Nikolov‡

*CSIRO Minerals, Seng.Lim@csiro.au

†CSIRO Process Science and Engineering, trevor.hadley@csiro.au

‡CSIRO Process Science and Engineering

This paper is posted at ECI Digital Archives.

http://dc.engconfintl.org/fluidization_xiii/21

UNDERSTANDING CAPTURE EFFICIENCY IN FLUIDIZED BEDS

Kok-Seng Lim, Jonian Nikolov, Trevor D. Hadley

CSIRO Process Science and Engineering
Bayview Avenue, Clayton, VIC 3168, Australia

ABSTRACT

This paper describes an experimental study on the extent of capture efficiency in a fluidized bed system under controlled conditions. Using aerosols as tracer compound, the capture efficiency in a fluidized bed was quantitatively measured as a function of contact distance (time). The paper presents the experimental technique as well as the results relating the capture efficiency to the bed hydrodynamic. A theoretical model was developed to describe the influence of operating variables on the overall capture efficiency. Dominant mechanisms enabling the capture of the fine aerosols are elucidated.

KEY WORDS

Fluidized bed filter, gas scrubbing, capture efficiency, gas-solid contactor, aerosols

INTRODUCTION

Fluidized beds have been used in a variety of chemical and physical processes due to the excellent gas-solid contact, heat and mass transfer characteristics. Typically, fluidized beds have widespread applications such as chemical reactors for chemical synthesis, mineral calcination, fuel combustion and gasification. As the particles in the fluidized bed provide large surface areas for fluid-particle and particle-particle contact, fluidized beds have also found applications in areas such as gas scrubbing, dust filtration and coating.

One example of fluidized bed gas scrubbing is the in-bed capture of sulphur dioxide gas (e.g. in coal combustors) by calcium containing minerals (1). The concept has been extended to pressurized fluidized bed combustion (PFBC) systems, where desulphurisation efficiency in excess of 90% have been achieved, thus minimising costly installation of additional flue gas scrubbing units (2).

Liu and Wey (3) and Liu et al (4) investigated the filtering characteristics of fluidized beds using coarse silica sand to capture coal combustion fly ash at various temperatures. Their studies found that the overall collection efficiency decayed with increasing operating time due to the effect of fly ash elutriation from the bed. The study highlighted the influence of various mechanisms including particle impact, diffusion, inter-particle forces, bounce-off effects and elutriation. The morphology and hardness of the particles were also found to play influencing roles in the capture efficiency. In another non-traditional fluidized bed system, Wang et al (5) used a magnetically stabilized fluidized bed to capture dust from flue gas under the influence of various variables such as magnetic field intensity, ratio of flue gas velocity to minimum fluidization velocity, bed height, and average particle size. Over

95% of dust removal was possible using this technique when the magnetic particles, acting as capture media, were refreshed regularly.

In a separate application, Yazbek and Delebarre (6) used a fluidized bed to capture volatile compounds by condensation effect. The capture efficiency was found to be influenced by the particle characteristics, temperature, bed height and fluidizing velocity. It was essential to minimise the effect of the liquid layer around the particles which would lead to defluidization and hence affect the fluidization quality. Furthermore by Ho et al (7) found that the chemisorption effect would also play a vital role for simultaneous capture of metal, sulphur and chlorine gases by sorbents in a fluidized bed incinerator. Recent work by Liu and Wey (8) extended the use of a fluidized bed for filtering nanoparticles from off-gas. They found some conflicting observations when comparing two different types of sorbent materials (silica sand and activated carbon). The authors attributed the differences to an additional diffusion effect when using more porous activated carbon.

Although fluidized beds offer promise for capturing gases and particulates such as dust, soot or aerosols, a fundamental understanding of the capture mechanisms is not always evident. Many of the studies were carried out in an environment where several mechanisms were at play, making it difficult to thoroughly elucidate the dominant capture mechanism.

The capture efficiency is known to be dependent on a number of factors including bed hydrodynamics, particle properties, inter-particle collision forces and adsorption kinetics. The mechanisms for the capture may be the result of particle interception, inertial impact, diffusion, gravitational settling, electrostatic attraction or chemisorption. Disruptive forces such as gas drag, particle collision and abrasion will lead to dislodgement of captured particles from the collecting media, reducing the overall capture efficiency.

The aim of this work is to provide a fundamental understanding of the capture mechanisms of aerosols in a fluidized bed from the bed hydrodynamic considerations. The work also permitted validation of a theoretical model so that the influences of various parameters on the capture efficiency could be evaluated and assist in optimising the fluidized bed design or operating parameters.

EXPERIMENTAL

An experimental system was set up to investigate the capture efficiency of aerosols (emulating one type of contaminants) in the fluidized bed under controlled conditions using a single injection approach for bubbles without the interaction of other effects. The experimental setup for the capture efficiency measurement (shown in Figure 1), is divided into three main parts: (1) an aerosol generator, (2) a fluidized bed for aerosol capture, and (3) a gas scrubbing system for the uncaptured off-gas. In the aerosol generator, a stream of aerosols (or fine droplets) is generated by an ultrasonic atomiser submerged in a salt (NaCl) solution (at concentration of 180 g/L). The aerosols, laden with salt solution, were acting as tracer compounds to assist determination of capture efficiency.

The aerosols, assisted by a carrier gas (air) were injected into a “two-dimensional” fluidized bed (295 mm wide, 450 mm tall and 18 mm deep bed) through a dedicated 12.5 mm ID tube at a pre-specified location. The flow rate of the carrier gas was adjusted between 3000 – 6000 cc/min using a rotameter (Fischer-Porter, Model F65, Tube A-250-5). The fluidized bed was equipped with a porous sintered brass plate and was fluidized separately by air to provide sufficient mixing of the bed particles and uniform capture of the tracer. Smelter grade alumina particles with mean particle size of $82 \pm 7 \mu\text{m}$ and particle density of 2770 kg/m^3 were used as bed material to capture the aerosols. The minimum fluidization velocity of the particles, U_{mf} , was estimated to be 0.007 m/s. A settled bed height of 200 mm was used for each experiment. Typically, the fluidized bed was fluidized with air at a superficial gas velocity of around 5.5 times the U_{mf} .

When injected into the bed, the aerosols dispersed in the gas bubbles would come in contact with and be captured by the surrounding particles in the emulsion phase. The uncaptured aerosols exiting from the fluidized bed were scrubbed in the gas scrubber system which was filled with fresh water (2.5 L) and pall rings to permit high efficiency scrubbing. The salt-laden aerosols dissolved quickly in the water and caused an increase in the conductivity of the wash solution. By continuously monitoring the conductivity of the scrubbing solution, it was possible to monitor the aerosol losses from the fluidized bed. The aerosol capture efficiency in the fluidized bed could be determined from the conductivity measurements. The conductivity of the water was measured using a conductivity meter (Oakton CON110). The conductivity readings were logged by a data logging system at 5-second time intervals. In addition, the bubbling flow behaviour was captured on video, so that the typical bubble sizes from the nozzle could be estimated.

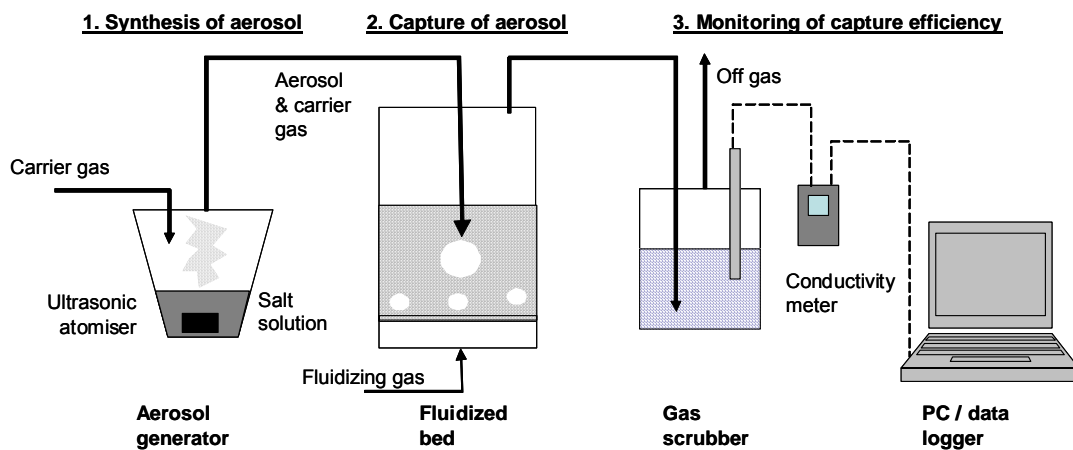


Figure 1. Experimental set up for aerosol capture efficiency study in fluidized bed.

RESULTS AND DISCUSSION

Experimental Results

The focus of this experimental study was to investigate the influence of contact distance (or time) on the overall capture efficiency of aerosols in the fluidized bed. The experiments were carried out by injecting aerosol-laden bubbles into the fluidized bed under a constant flow of carrier gas at different depths below the bed surface. Figure 2 shows the transient responses of the ionic conductivity of the scrubber solution as a function of time for the different injection bed depths. The increase of the conductivity in the scrubber solution is proportional to the loss of aerosol capture in the fluidized bed. As expected, the slope of the conductivity plot obtained for the reference conductivity curve (obtained with the empty bed) is greater than those obtained in experiments with bed solids. The change of conductivity in the scrubber solution provided an indirect measure of the overall capture efficiency, η_{expt} , of the aerosol in the fluidized bed which can be conveniently expressed by the following equation,

$$\eta_{expt} = 1 - m_{expt} / m_{ref} \quad [1]$$

Where:

- m_{ref} is the slope of conductivity plot shown in Figure 2 as determined in an empty bed (without bed particles) and;
- m_{expt} is the slope of conductivity plot from the experiment conducted in the fluidized bed containing bed particles.

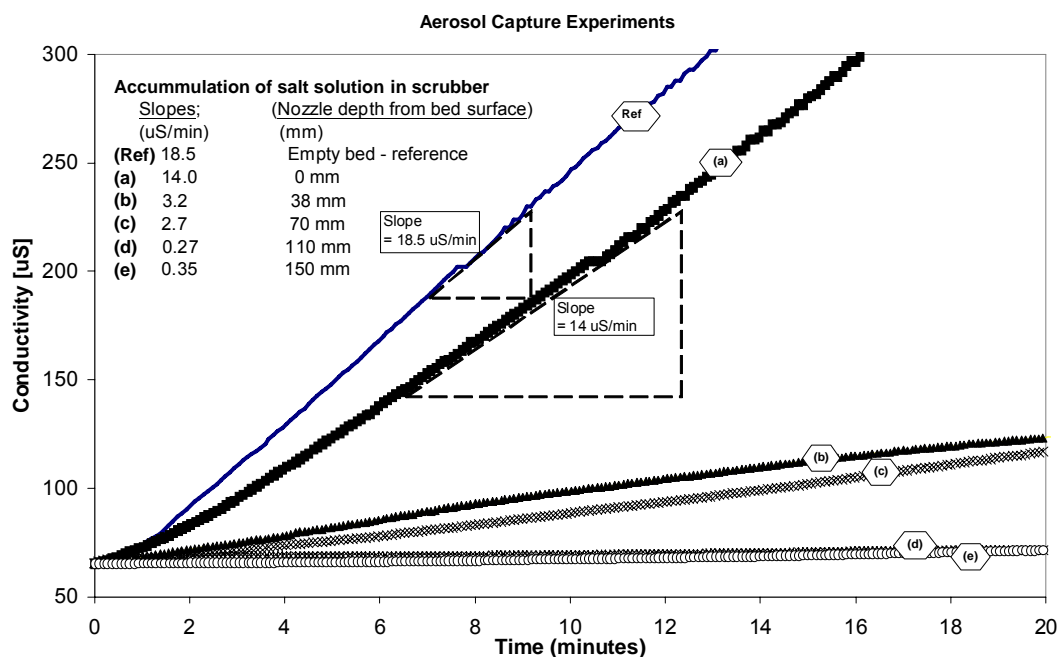


Figure 2. Conductivity readings of the scrubber solution as a means to monitor the overall capture efficiency in the fluidized bed. Measurements were conducted at different injection locations. Carrier gas flow rate was 3000 cc/min.

The overall capture efficiencies of the aerosols were calculated using equation [1]. Figure 3 shows the capture efficiency curve plotted as a function of injection nozzle depth, representing different contact distances. The capture efficiency was found to increase rapidly with increasing contact distance, which provided a greater

opportunity for the aerosols to interact with the bed solids. Under the conditions studied, a capture efficiency in excess of 95% was observed for a contact distance of 150 mm.

Theoretical Modelling

To support the above study, a theoretical model was developed to describe the capture mechanism in the fluidized bed based on a single bubble injection condition. In this model, it is theorised that the gas (including the dispersed tracer compound) in the bubble is in constant exchange with the surrounding particles through the bubble-emulsion interface or boundary. The interchange between the bubble and bubble cloud involves both bulk flow and diffusion as shown in the inset of Figure 3. The mass balance for the tracer in a single rising bubble can be described as follows, according to Kunii and Levenspiel (9):

$$-V_b dC_b/dt = (q + k_{bc}S_{bc})(C_b - C_c) \tag{2}$$

Where q is bulk flow through the bubble and k_{bc} is the mass exchange coefficient between the bubble and the cloud phase, which can be expressed as follows (9).

$$q = 3\pi U_{mf} d_b^2 / 4 \tag{3}$$

$$k_{bc} = 0.975 \mathcal{D}^{0.5} (g/d_b)^{0.25} \tag{4}$$

The mechanism for the capture is due to aerosols impacting and physical adsorption with the surrounding particles during the exchange of flow. The resultant concentration of aerosol in the cloud phase after capture may be defined as follows:

$$C_c = C_b \varepsilon_{mf} \chi \tag{5}$$

Where χ is the adhesion propensity of the aerosols onto the colliding particles, which in this case is assumed to be complete, i.e. $\chi=1$.

By substituting equations [3-5] into equation [2] and then followed by integration, it is possible to describe the tracer concentration in the bubble C_b as a function of time. Rearranging the integral solution, a theoretical capture efficiency, η_{th} , can be expressed as follows,

$$\eta_{th} = (C_{b,0} - C_b) / C_{b,0} = 1 - \exp(-(q + k_{bc}S_{bc})(1 - \varepsilon_{mf} \chi)t / V_b) \tag{6}$$

Where $C_{b,0}$ is the initial concentration of tracer in the bubble phase.

Table 1. Revelant parameters used in the theoretical model for capture efficiency.

Parameters	Comments
$d_b = 2.5 \text{ cm}$	As determined from the video images during the experiments.
$\varepsilon_{mf} = 0.42$	Emulsion voidage.
$U_b = K\sqrt{gd_b}$	Where $K=0.5$ for ‘two-dimensional’ bubbles (11).
$\mathcal{D} = 7.0E-5 \text{ m}^2/\text{s}$	It is assumed that the following relationship holds: $\mathcal{D} = \text{“} \mathcal{D}_{\text{aerosol}} \text{”} = m \times \mathcal{D}_{\text{air-heavy gas system}}$ The diffusion coefficient for aerosols is assumed to be a similar order of magnitude as that in an air-heavy gas system (e.g., air-ethyl acetate system) where $\mathcal{D}_{\text{air-heavy gas system}} = 7E-06 \text{ m}^2/\text{s}$ (10). For highly adsorptive system, m value up to 10 has been suggested (9, page 245) which is used here.

The theoretical capture efficiency (equation [6]) is shown to be related to the hydrodynamic phenomena. For validation purposes, the predicted capture efficiency values are compared with the experimental data as shown in Figure 3. The contact time, t , used in equation [6] is related to contact distance (Z), based on the relationship $Z = U_b t$, where U_b is the bubble rise velocity. Other parameters used in the model are summarized in Table 1.

As shown in Figure 3, the predicted capture efficiency provided good agreement with the experimental data. The model predicted a similar trend showing rapid increase of capture efficiency with increasing contact distance. The capture efficiency reaches an asymptote at a bed depth around 150 mm, similar to that observed in the experiment. From the agreement, it could be construed that the proposed mechanisms of contact and capture used in the model are reflective of physical process.

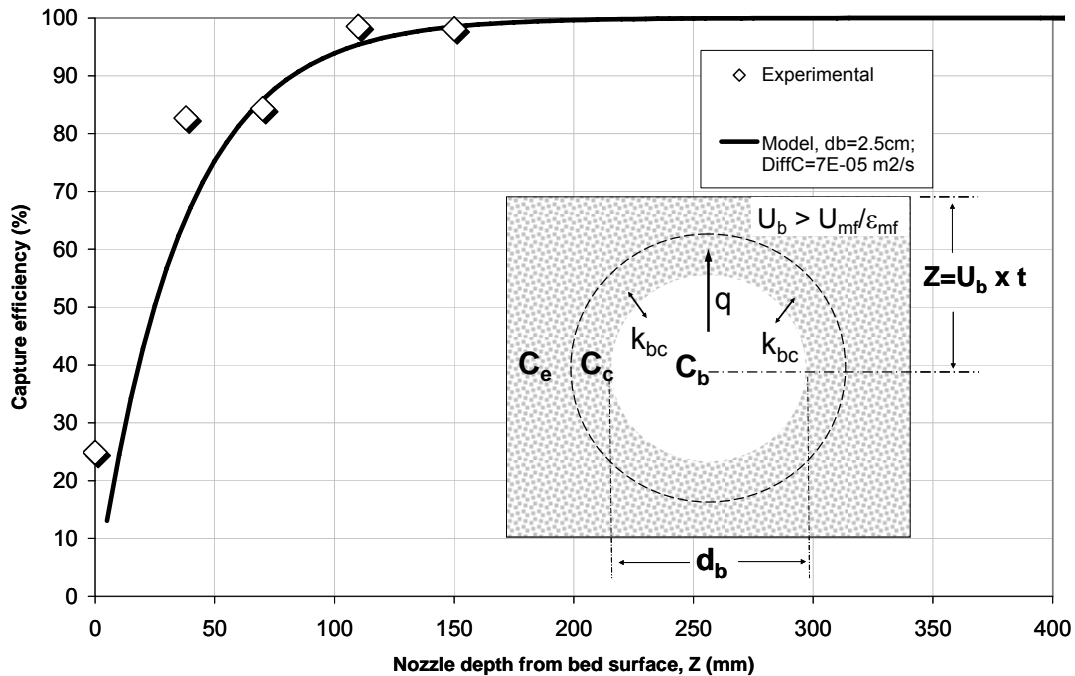


Figure 3. Capture efficiency in the fluidized bed as a function of contact distance (from the injection nozzle tip to the bed surface) and compared with theoretical prediction (carrier gas flow rate = 3000 cc/min). Inset: schematic showing the flow exchange between the bubble and its surrounding.

Further modelling studies were conducted to examine the sensitivity of various operating parameters on the overall capture efficiency. Figure 4a shows the effect of bubble size on the capture efficiency. The capture efficiency is noticeably lower if the bubble size is increased, due to bubble by-passing effect. This trend is also expected if the gas velocity is increased or using particle size classification that would lead to large bubbles. To achieve high capture efficiency, the bubble size should be maintained as small as practically possible or using internal baffles to break up bubbles. Alternatively, the contact distance can be increased but at the expense of increased pressure drop; hence higher energy consumption.

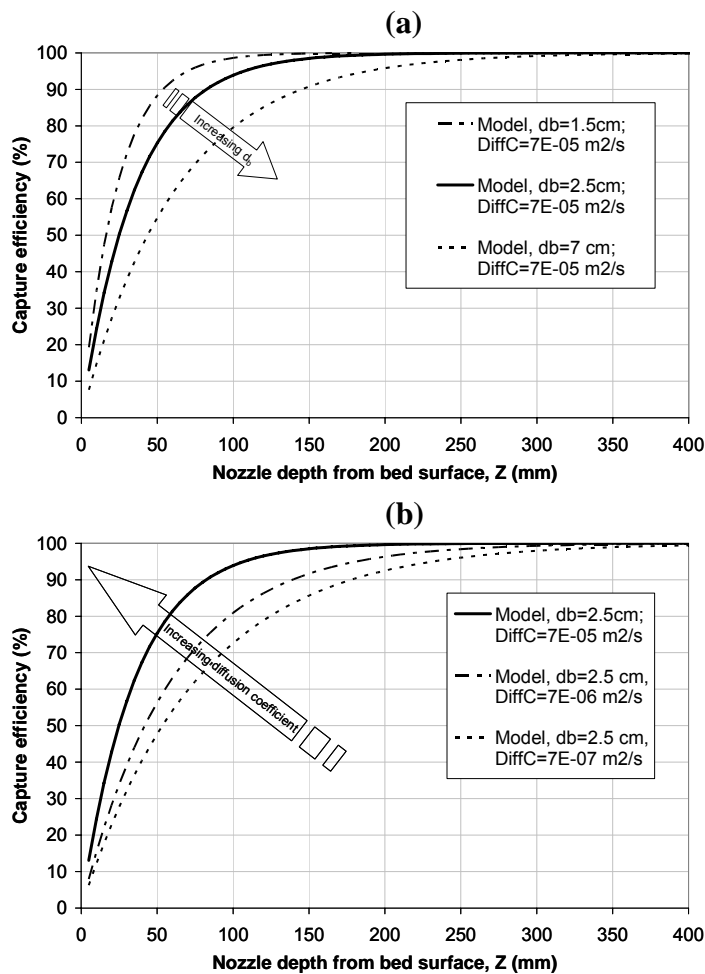


Figure 4. Capture efficiency in the fluidized bed due to the effects of (a) bubble size (2D system) (b) diffusion coefficient.

The theoretical model based on single bubble injection has provided useful insights into the underlying mechanisms controlling the capture efficiency in the fluidized bed. It can be extended to a bubble swarm system to predict likely capture efficiency in a larger scale fluidized bed contactor. In the case of capturing fine particles in fluidized bed, additional mechanisms such as elutriation and abrasion can be incorporated.

CONCLUSIONS

This study has successfully designed and tested an experimental technique, using a salt-laden aerosol tracer, to examine the extent of capture efficiency in a fluidized bed system under controlled conditions. The capture efficiency was found to be related to the bed hydrodynamics which was explained through a theoretical model. The mechanism for the capture is due to aerosols impacting with the surrounding particles during the exchange of flow in the bubbles consisting of convective flow and diffusion. Key operating parameters influencing the performance of a fluidized

Simulations shown in Figure 4b examine the effect of the diffusion coefficient on the capture efficiency. This parameter is related to the types of contaminants used (gases, aerosols or particulates). It is shown that the bed achieves greater capture efficiency if the diffusion coefficient is larger. Highly adsorptive gases or aerosols would also lead to a larger effective diffusion coefficient. The adhesion/absorption propensity of the sorbent is also important when considering capture efficiency, which is not hydro-dynamically controlled. Though not presented here, the influence of sorbent on capture could be characterised by the factor χ in the model.

bed to capture aerosol contaminants are identified, providing useful guidelines for optimising the fluidized bed contactor design and operating parameters.

ACKNOWLEDGEMENTS

The authors would like to acknowledge the contributions of Dr John Sanderson and Mr Hengky Sidharta in the early stage of the study.

NOTATION

C_b = tracer concentration in bubble phase (-)	U_{mf} = minimum fluidization velocity (m/s)
C_c = tracer concentration in cloud phase (-)	U_b = bubble rise velocity (m/s)
$C_{b,0}$ = initial tracer concentration in bubble phase (-)	V_b = volume of the bubble (m ³)
d_b = bubble diameter (m)	Z = distance between nozzle entry to bed surface (m)
g = gravitational acceleration (m/s ²)	
k_{bc} = mass exchange coefficient between the bubble and the cloud (m/s)	Greek symbols
K = constant for bubble rise velocity (-)	χ = adhesion factor (-)
q = bulk flow through the bubble (m ³ /s)	\mathcal{D} = effective diffusion coefficient (m ² /s)
S_{bc} = interfacial area of bubble to cloud (m ²)	ε_{mf} = voidage at minimum fluidization condition (-)
t = contact time (s)	η = capture efficiency (-)

REFERENCES

1. S. Boskovic, B.V. Reddy and P. Basu, Effect of operating parameters on sulphur capture in a pressurized circulating fluidized bed combustor, *Int. J. Energy Res.*, **26** (2002) 173-183.
2. E.J. Anthony and D.L. Granatstein, Sulfation phenomena in fluidized bed combustion systems, *Progress in Energy and Combustion Science*, **27** (2001) 215-236.
3. K.Y. Liu, M.Y. Wey, Filtration of fly ash using fluidized bed at 300-500°C, *Fuel* **86** (2007) 161-168.
4. K.Y. Liu, J.Y. Rau and M.Y. Wey, Collection of SiO₂, Al₂O₃ and Fe₂O₃ particles using a gas-solid fluidized bed filter, *J. Hazardous Materials*, **171** (2009) 102-110.
5. Y. Wang, K. Gui, M. Shi and C. Li, Removal of dust from flue gas in magnetically stabilized fluidized bed, *Particuology* **6** (2008) 116-119.
6. W. Yazbek and A. Delebarre, Separation of volatile compounds by condensation in a fluidized bed, *Chem. Eng. Sci.*, **60** (2005) 577 - 588.
7. T.C. Ho, T.C. Chuang, S. Chelluri, Y. Lee and J.R. Hopper, Simultaneous capture of metal, sulphur and chlorine by sorbents during fluidized bed incineration, *Waste Management*, **21** (2001) 435-441.
8. K.Y. Liu and M.Y. Wey, Filtration of nano-particles by a gas-solid fluidized bed, *J. Hazardous Materials*, **147** (2007) 618-624.
9. D. Kunii and O. Levenspiel, *Fluidization Engineering*, Butterworth-Heinemann, 2nd Ed, Boston (1991).
10. N.H. Chen and D.F. Othmer, New generalised equation for gas diffusion coefficient, *J of Chem Eng Data*, **7** (1962) 37-41.
11. K.S. Lim and P.K. Agarwal, Bubble velocity in fluidized beds: The effect of non-vertical bubble rise on its measurement using submersible probes and its relationship with bubble size, *Powder Technology*, **69** (1992), 239-248.